Structural Engineering and Mechanics, *Vol. 52, No. 6 (2014) 1225-1256*
DOI: http://dx.doi.org/10.12989/sem.2014.52.6.1225

Design charts for yield acceleration and seismic displacement of retaining walls with surcharge through limit analysis

Mohamad Mahdi Aminpoor* and Ali Ghanbari[a]

Faculty of Engineering, Kharazmi University, No. 49 Mofatteh Ave., Tehran, I.R. Iran

(Received June 18, 2013, Revised June 26, 2014, Accepted October 2, 2014)

Abstract. Calculating the seismic displacement of retaining walls has an important role in the optimum design of these structures. Also, studying the effect of surcharge is important for the calculation of active pressure as well as permanent displacements of the wall. In this regard, some researchers have investigated active pressure; but, unfortunately, there are few investigations on the seismic displacement of retaining walls with surcharge. In this research, using limit analysis and upper bound theorem, permanent seismic displacement of retaining walls with surcharge was analyzed for sliding and overturning failure mechanisms. Thus, a new formulation was presented for calculating yield acceleration, critical angle of failure wedge, and permanent displacement of retaining walls with surcharge. Also, effects of surcharge, its location and other factors such as height of the wall and internal friction angle of soil on the amount of seismic displacements were investigated. Finally, designing charts were presented for calculating yield acceleration coefficient and angle of failure wedge.

Keywords: retaining wall; seismic displacement; limit analysis; surcharge; design charts

1. Introduction

Studying the behavior and seismic response of earth retaining structures is very important owing to the economic gain of their design in terms of damage mitigations of big earthquakes. Evidence of earthquake-induced damages to retaining structures is widely documented (e.g., Pitilakis and Moutsakis 1989, Tateyama *et al*. 1995, Fang *et al*. 2003, Huang and Chen 2004, Trandafir *et al*. 2009). Many of the available techniques for seismic analysis of retaining walls such as Mononobe-Okabe (1929, 1924) provide useful information about the active earth pressure. However, the applicability of these walls after earthquake highly depends on their deformations during the quake. In fact, active horizontal pressure behind the walls depends on the amount of displacements as well as direction of wall's movement (Wu and Prakash 2001).

Newmark (1965) considered a rigid failure wedge and calculated the acceleration required to result in a unit factor of safety for stability of the slope based on the limit equilibrium theorem. Using this acceleration, permanent displacement for the desired failure wedge was calculated. Richards and Elms (1979) proposed a simple approach based on sliding block of Newmark for

*Corresponding author, Ph.D. Student, E-mail: Aminpoor32@gmail.com
[a]Associate Professor, E-mail: Ghanbari@khu.ac.ir

http://www.techno-press.org/?journal=sem&subpage=8 ISSN: 1225-4568 (Print), 1598-6217 (Online)

dynamic design of rigid retaining walls. Wu (1999) proposed mathematical models for determination of walls' displacements by considering dry and submerged soil. Using the finite element method, Nadim (1982) and Nadim and Whitman (1983) studied the displacements of retaining walls. Based on their studies, seismic pressure applied to the walls might be greater than 30% of the active earth pressure in the static conditions. Whitman and Liao (1985) identified the errors in the method of Richards and Elms (1979) and explained the error by a normal logarithmic distribution.

Huang (2006) expressed the seismic displacement of two common types of bridge abutments in Taiwan by pseudo-static method based on multi-wedge theory. He concluded that the presence of backfill in front of the abutment had an important role in the reduction of seismic displacements. Michalowski (2007) obtained the displacement of earth slopes due to seismic triggers by Kinematic approach of limit analysis and concluded that, in the soils that followed the non-associated flow rule, failure acceleration was smaller than the soils following the associated flow rule.

Huang *et al*. (2009) calculated the seismic displacement of common walls based on a series of shaking table experiments as well as analytical modeling, called multi wedge pseudo-static method, based on the sliding block of Newmark (1965). Their results showed that the ratio of horizontal displacements to height of the wall usually varied between 2% and 5%, which included the range of ordinary displacements to extensive damage failure of the wall. Finally, they suggested that the maximum seismic displacement of retaining walls in non-cohesive soils was about 5% of the wall height.

Using limit equilibrium theorem, Trandfir *et al*. (2009) estimated the sliding failure displacement and rotational failure displacement of retaining walls and also calculated rotational failure displacements for reinforced embankments. According to their studies, vertical and horizontal seismic displacements of the crown of reinforced embankments were about 12% and 32% smaller than the seismic vertical and horizontal displacement of the crown of failure wedge behind the walls, respectively.

Stamatopoulos *et al*. (2006), Biondi *et al*. (2013) proposed solutions for the evaluation of a wall displacement factor embodying all the geometrical and mechanical characteristics of the soil-wall system and enabling to obtain the wall displacement through a simple sliding block analysis.

Li *et al*. (2010) studied the stability of gravity retaining walls by upper bound limit analysis technique. In this method, retaining wall and its backfill are considered a complete system. Using the limit equilibrium technique and upper bound theorem, Mojallal and Ghanbari (2012) calculated the angle of failure wedge, yield acceleration, and permanent displacements of retaining walls in seismic conditions for sliding and sliding-rotational failure mechanisms. In recent years, several studies have been devoted to studying the seismic stability of slopes and retaining walls (Michalowski 1998a, You and Michalowski 1999, Michalowski and You 2000, Sadrekarimi *et al*. 2008, Michalowski 2010, Anastasopoulos *et al*. 2010, Gursoy and Durmus 2009, Haciefendioglu *et al*. 2010, Kim *et al*. 2008, Cocco *et al*. 2010).

Stress plasticity solutions for evaluating earth pressure coefficients have been proposed by Mylonakis *et al*. (2007), Evangelista *et al*. (2010). Mylonakis *et al*. (2007) derived closed-form solutions for evaluating static and pseudo-static earth pressure coefficients under both active and passive conditions. Evangelista *et al*. (2010) proposed a solution for evaluating active earth pressures on cantilever retaining walls with a long foundation heel and showed that, in seismic conditions, the inclination of the active thrust to the horizontal was larger than that in static conditions. A closed-form solution to the specific problem was presented by Kloukinas and

Mylonakis (2011).

There are very few studies on the relation between displacement of retaining walls in the presence of a surcharge. Motta (1994) proposed closed-form expressions of the seismic active earth pressure coefficient accounting for the presence of a distanced surcharge on the backfill soil; Caltabiano *et al*. (1999), Caltabiano *et al*. (2000) provided coupled solutions for the critical acceleration coefficient and the angle of the failure plane of walls with (Caltabiano *et al*. 2000) or without (Caltabiano *et al*. 1999) a distanced surcharge; Caltabiano *et al*. (2005), who proposed a procedure for seismic design of retaining walls accounting for the actual failure mechanism mobilized in limit equilibrium conditions and also distinguishing the contributions of the earth thrust and of the inertia of the soil wedge in the evaluation of the actual driving moments to be considered in the equilibrium against rotation. Greco (2006) calculated the active force applied to the retaining walls in seismic and static conditions in the presence of a series of linear surcharges by limit equilibrium method. Ghanbari and Taheri (2012) calculated active pressure for reinforced retaining walls due to linear surcharge based on horizontal slices method.

Biondi *et al*. (2009) presented a general coupled limit equilibrium solution for the yield acceleration and of the critical angle of the plastic wedge of walls subjected to a distanced uniform surcharge accounting also for backfill and wall internal face inclination, for soil-wall friction and vertical component of the seismic loading. Using limit equilibrium technique, Caltabiano *et al*. (2012) calculated the angle of failure and critical acceleration as well as coefficient of active pressure to retaining walls in the presence of various surcharges for static and seismic conditions. Varzaghani and Ghanbari (2014) calculated the displacement of slopes subjected to a distanced limited dynamics surcharge.

In this paper, using the principles of limit analysis theorem, seismic displacement of retaining walls was estimated in the presence of a surcharge. For this purpose, first, yield acceleration was calculated for different types of surcharge. Then, using the sliding wedge theory of Newmark, the amount of permanent displacement for sliding and rotational mechanisms was estimated. Finally, design charts were presented based on the suggested technique.

2. Limit analysis

Finding analytical solutions for practical engineering soil and rock mechanics problems is, however, a difficult task. Finn (1967), Chen (1975), Chen and Liu (1990) have presented purely analytical applications of limit analysis to some practical geotechnical problems (Durand *et al*. 2006). Limit analysis is an approach to stability calculations based on two theorems that make it possible to find upper and lower bounds to unknown quantities, such as the critical height of a slope, bearing capacity of foundations, etc. Alternatively, for given structures and given loads an estimate of material parameters necessary to maintain stability can be found (Michalowski 1998b). Lower and upper bound estimates of the collapse load factor can be obtained by both analytical and computational methods. In the case of lower bound solutions, statically admissible stress fields have to be assumed, whereas in the case of upper bound solutions, a kinematically admissible velocity field must be assumed. In the latter case, this can be done by establishing a failure mechanism.

The lower bound theorem in its general form was then independently established by Feinberg (1948) and proved by Hill (1948) by applying the principle of maximum plastic work to a finite volume of perfectly plastic material. A more complete statement of both lower and upper bound

theorems and their proof has presented by Hill (1951) three years later. Drucker *et al*. (1952) first noted that the stress state remains constant at plastic collapse and threfore proved that the lower and upper bound theorems of limit analysis are also valid for elastic-plastic materials (Yu 2006).

The upper bound theorem, which uses a rigid perfectly plastic soil model, states that the internal energy dissipated by any kinematically admissible velocity field can be equated to the work done by external loads, and so enables a strict upper bound on the actual solution to be deduced. The lowest possible upper bound solution is sought with an optimization scheme by trying various possible kinematically admissible fracture surfaces. A kinematically admissible velocity field is the one that satisfies compatibility, a plastic flow rule and the velocity boundary conditions (Yang 2007). It is useful to write this theorem in a mathematical form

$$\int \sigma_{ij}^{k} \dot{\varepsilon}_{ij}^{k} dV \geq \int_{S} T_i V_i dS + \int_{V} X_i V_i^{k} dV \tag{1}$$

In this equation, the left-hand side is the rate of the internal work or energy dissipation and in the right hand sight the first term shows the unknown distributed load on boundary S and the second term shows the work rate of the distributed forces per unit volume such as weight or inertial forces. Distributed loads on boundary S moving with velocity V_i (kinematic boundary condition) and distributed forces per unit volume related to thekinematically admissible velocity field V_i^k. σ_{ij}^k is the stress state which is in agreement with selected mechanism (Michalowski 2007). The strain rate $\dot{\varepsilon}_{ij}^k$ represents any set of strains or deformations compatible with real or virtual displacement rate V_i or V_i^k of the points of the applications of the external forces T_i or body forces X_i (Chen 1975).

3. Basic assumptions in the proposed technique

The proposed formulation of this research was based on kinematic limit analysis and upper bound theorem. The assumptions were as follows:

1. Failure wedge was considered as a single planar block.
2. The Newmark's sliding block method was used to estimate seismic displacements.
4. Retaining wall was assumed to be a rigid gravity wall which can tolerate sliding and rotational movements.
3. Backfill soil was dry and cohesionless and followed the associated flow rule as well as the Mohr-Coulomb failure criterion.
4. The wall was assumed to be either gravity retaining wall or cantilever retaining wall. Two types of sliding and overturning failure mechanisms were considered for the analyses.
5. Surcharge was static. It was applied at a certain distance from the end of the wall.

4. Proposed formulation for calculating yield acceleration coefficient

In order to calculate yield acceleration coefficient, three different conditions were considered with regard to the location of surcharge:

1. Surcharge was completely located inside the failure wedge.
2. A part of surcharge was inside the failure wedge and the rest of it was located outside.

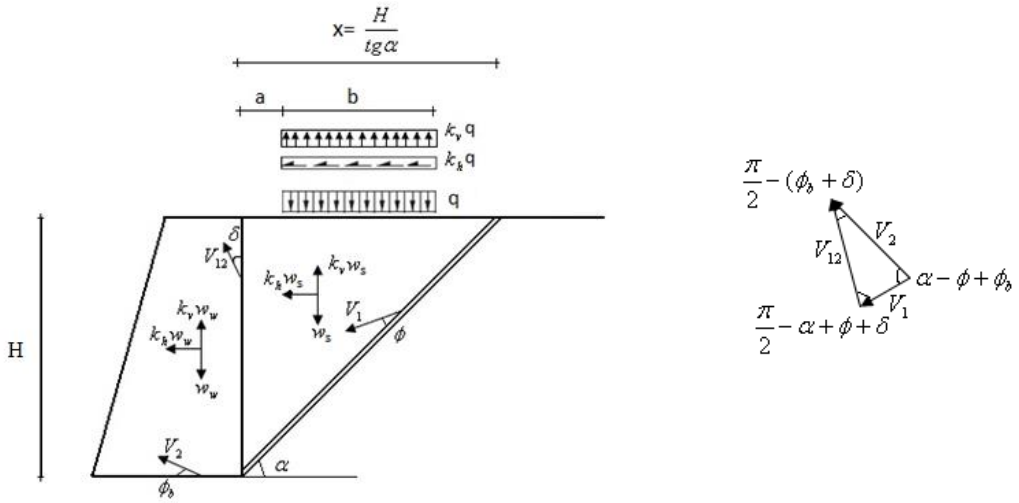

(a) Incipient velocities (b) Hodograph of the velocity

Fig. 1 Initial single-block failure mechanism for the first case (surcharge completely inside the failure wedge)

3. Surcharge was completely located outside the failure wedge.

The used mechanism as well as applied forces for the first condition where the surcharge was completely located inside the failure wedge is illustrated in Fig. 1.

In Fig. 1, V_1 and V_2 are velocity vectors of the failure wedge and retaining wall, respectively, and V_{12} is the relative velocity between the wall and failure wedge. Based on the associated flow rule, the sliding vector, V_1, makes the angle of φ with the failure surface. Also, the sliding vector, V_{12}, makes the angle of δ with the direction of wall, and the sliding vector, V_2, makes φ_b angle with the wall's direction and the soil underneath the wall.

Rate of internal work or dissipated energy $(\dot{D})$ is determined by Eq. (2)

$$\dot{D} = \frac{\mathrm{cH}}{\sin\alpha}\mathrm{V}_1\cos\phi \tag{2}$$

where c is soil cohesion which is assumed to be zero.

In this condition, rate of external work due to body forces including weight of the failure wedge, weight of the wall, and rate of the work done by external forces due to surcharge (traction) can be obtained by Eqs. (3), (4), and (5), respectively.

$$\dot{W}_s = \mathrm{K_h} W_s V_1 \cos(\alpha-\phi) + (1-k_v)(W_s V_1 \sin(\alpha-\phi)) \tag{3}$$

$$\dot{W}_w = \mathrm{K_h} W_w V_2 \cos(\phi_b) - (1-k_v)(W_w V_2 \sin(\phi_b) \tag{4}$$

$$\dot{Q}_1 = \mathrm{K_h} qbV_1 \cos(\alpha-\phi) + (1-k_v) qbV_1 \sin(\alpha-\phi) \tag{5}$$

Based on the upper bound theorem of limit analysis and Eq. (1), rate of the internal work must be greater than or equal to the external work.

$$\dot{D} \geq (\dot{W}_s + \dot{W}_w) + \dot{Q}_1 \tag{6}$$

With regard to Fig. 1(b), it can be written

$$d = \frac{V_1}{V_2} = \frac{\cos(\phi_b + \delta)}{\cos(\alpha - \phi - \delta)} \tag{7}$$

Assuming that the ground acceleration reached the yield acceleration at the time of failure (k_y=k_h), the following can be written

$$\dot{D} = (\dot{W}_s + \dot{W}_w) + \dot{Q}_1 \tag{8}$$

Considering the following parameters, yield acceleration coefficient can be obtained by Eq. (9).

$$K_{y1} = \frac{A_1}{\lambda A_1 - A_2} \tag{9}$$

$$A_1 = W_s d \sin(\alpha - \phi) + qbd \sin(\alpha - \phi) - W_w \sin(\phi_b) \tag{10}$$

$$A_2 = W_s d \cos(\alpha - \phi) + qbd \cos(\alpha - \phi) + W_w \cos(\phi_b) \tag{11}$$

$$\lambda = \frac{K_v}{K_h}, W_s = \frac{H^2}{2\tan(\alpha)} \tag{12}$$

where W_w is weight of wall and W_s is weight of failure wedge.

In conventional analyses, inclination angle, α, is usually given. In order to obtain the best estimation (i.e., the least upper bound), failure angle has to be calculated which leads to the minimum yield acceleration in the structure. Therefore, yield acceleration coefficient is maximized with regard to α. Therefore, the following can be written

$$\frac{\partial K_y}{\partial \alpha} = 0 \tag{13}$$

Solving Eqs. (9) and (13) simultaneously using trial and error method leads to obtaining the angle of critical failure wedge and minimum yield acceleration coefficient. It should be noted that identical solutions have been obtained by closed-form analytical formulations derived in the framework of limit equilibrium in previous studies (e.g., Caltabiano *et al*. 2000, 2012).

As shown in Fig. 2, in the second condition, only a part of surcharge was inside the wedge. In this case, rate of the work done by body forces was the same as the previous condition. However, the work done by traction forces due to the loading can be obtained by Eq. (14). Also, yield acceleration coefficient can be obtained by Eq. (15). Similar to the previous case, solving Eqs. (13) and (15) simultaneously led to the angle of critical failure wedge and minimum yield acceleration coefficient.

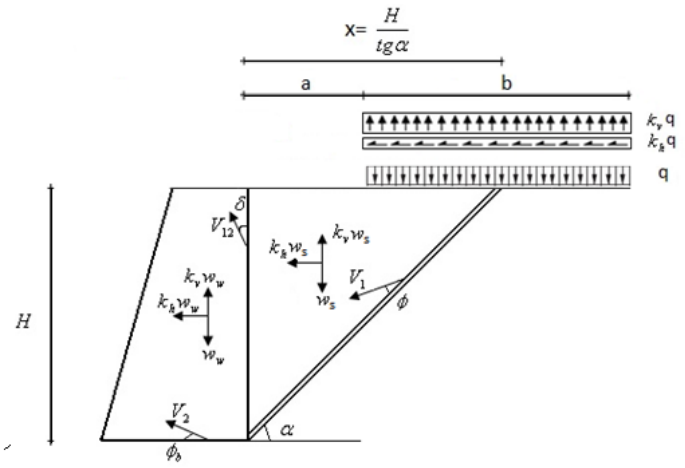

Fig. 2 Initial single block failure mechanism and incipient velocities for the second condition (a part of surcharge inside the failure wedge)

$$\dot{Q}_2 = (1-K_v)\left[q\left(\frac{H}{\tan(\alpha)}-a\right)V_1\sin(\alpha-\phi)\right]+K_h q\left(\frac{H}{\tan(\alpha)}-a\right)V_1\cos(\alpha-\phi) \tag{14}$$

$$K_{y2}=\frac{A_3}{\lambda A_3 - A_4} \tag{15}$$

$$A_3 = W_s d\sin(\alpha-\phi)+q\left(\frac{H}{\tan(\alpha)}-a\right)d\sin(\alpha-\phi)-W_w\sin(\phi_b) \tag{16}$$

$$A_4 = W_s d\cos(\alpha-\phi)+q\left(\frac{H}{\tan(\alpha)}-a\right)d\cos(\alpha-\phi)+W_w\cos(\phi_b) \tag{17}$$

In the third condition, where the surcharge was outside the failure wedge, rate of the work done by body forces was similar to the previous cases. However, the work done by traction forces due to the loading was equal to zero. In this case, yield acceleration coefficient was obtained by Eq. (18). Minimum yield acceleration coefficient can be obtained by simultaneously solving Eqs. (13) and (18).

$$K_{y3}=\frac{A_5}{\lambda A_5 - A_6} \tag{18}$$

$$A_5 = W_s d\sin(\alpha-\phi)-W_w\sin(\phi_b) \tag{19}$$

$$A_6 = W_s d\cos(\alpha-\phi)+W_w\cos(\phi_b) \tag{20}$$

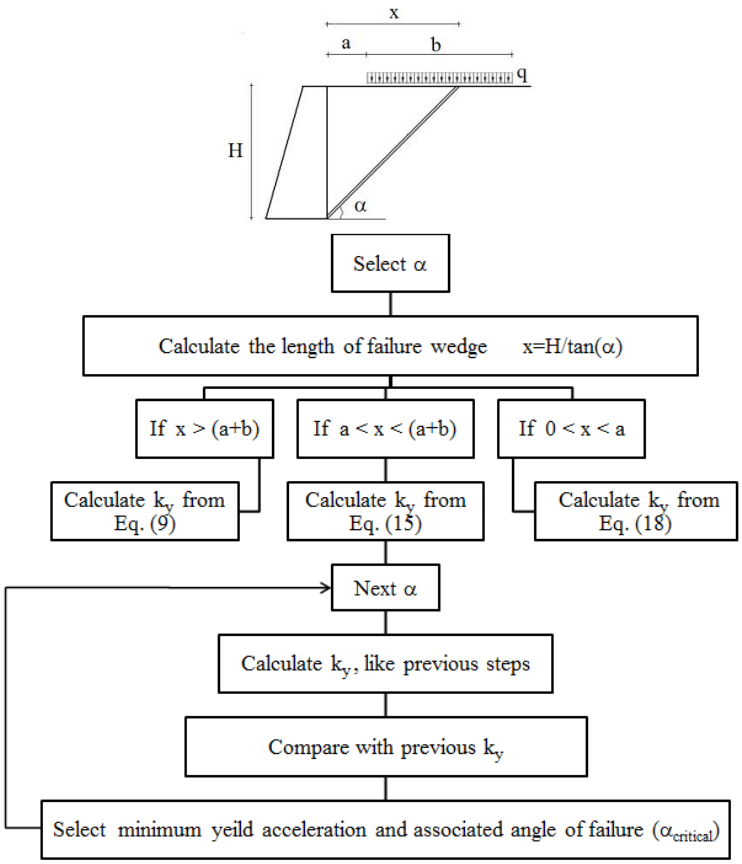

Fig. 3 Algorithm for calculating the yield acceleration coefficient for a retaining wall based on the proposed method

In order to calculate k_y, numerical methods using the algorithm shown in Fig. 3 can be used. Therefore, by writing codes in a programming language, minimum yield acceleration coefficient can be obtained for various conditions of surcharge.

5. Results for yield acceleration coefficient

In this section, behavior of the retaining walls for various conditions of wall and backfill as well as intensity and location of surcharge is studied. Considering the proposed formulation, length of the failure wedge and location of surcharge were the effective parameters for minimizing yield acceleration. Fig. 4 shows the effect of the distance of surcharge from the wall edge on the yield acceleration coefficient. By increasing the distance of the surcharge from the wall, the surcharge effect finally disappeared and the wall performed as the case without the surcharge. Also, Fig. 5(a) and (b) shows the variations in angle of failure wedge and length of failure wedge versus the distance of surcharge from the wall edge. With regard to these figures, variations of yield acceleration with regard to failure wedge were obvious.

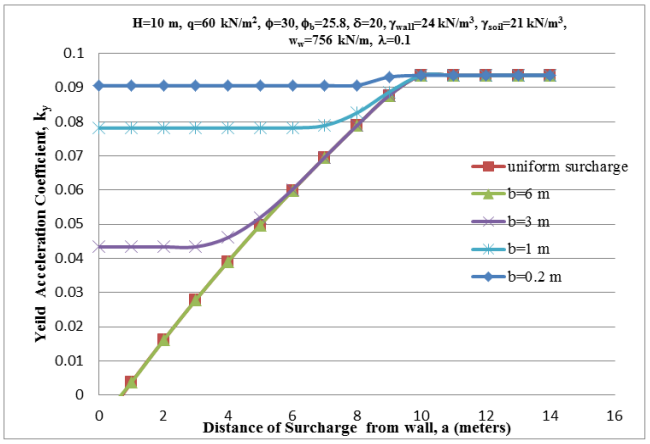

Fig. 4 Variations of the yield acceleration coefficient with regard to the distance of surcharge from the wall end for different widths of surcharge

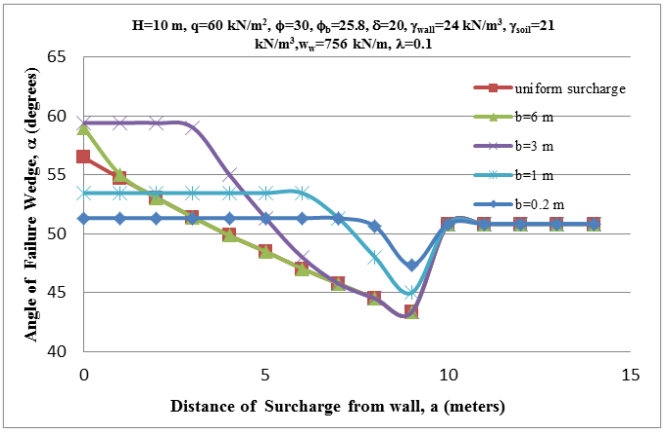

(a)

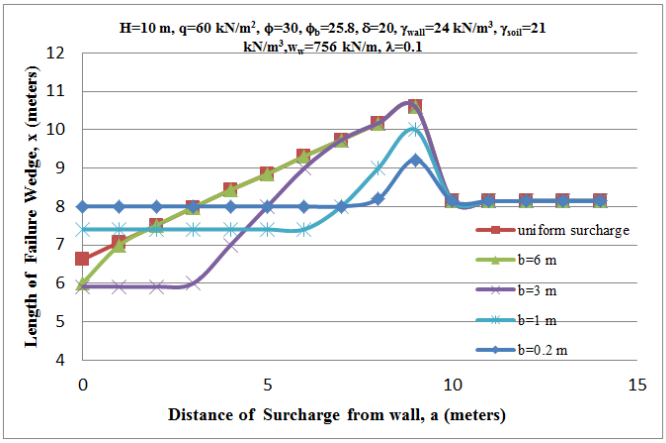

(b)

Fig. 5 (a) Variations of angle of failure wedge, (b) Variations of length of failure wedge with regard to the distance of surcharge from the wall end for different widths of surcharge

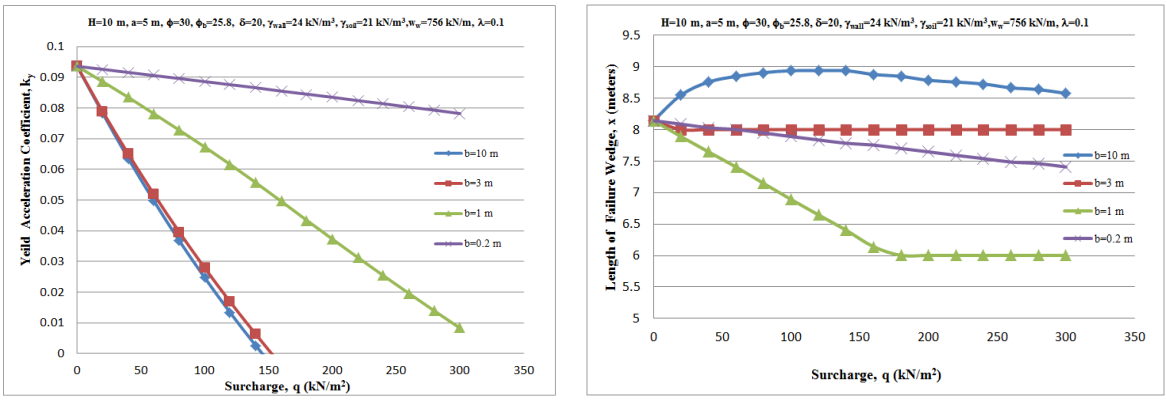

(a) (b)

Fig. 6 (a) Variations of yield acceleration, (b) Variations of the length of failure wedge versus the surcharge intensity for various geometries of surcharge

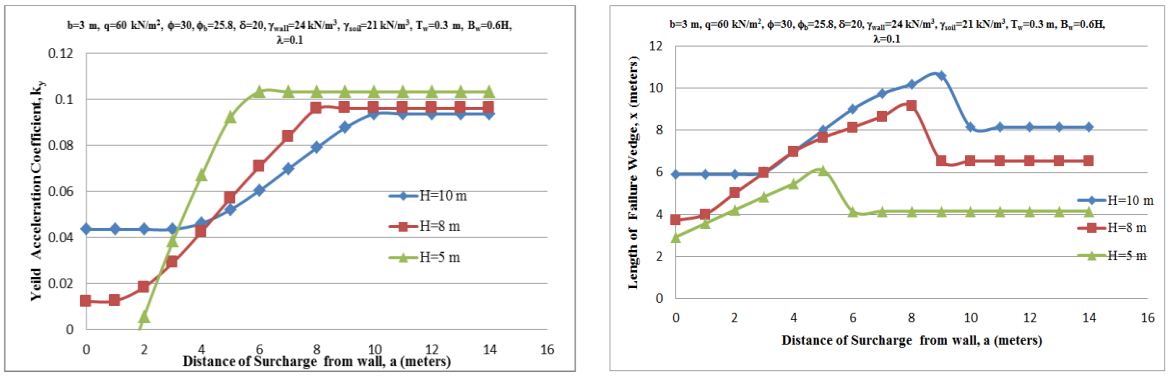

(a) (b)

Fig. 7 (a) Variations of the yield acceleration, (b) Variations of the length of failure wedge along the height of wall for different distances of surcharge from the wall

Variations of the yield acceleration coefficient against the surcharge intensity are illustrated in Fig. 6(a). Based on the obtained results, an increase in the intensity of surcharge caused a decrease in the yield acceleration coefficient to the point that, for the surcharges with high intensity, k_y was zero. Condition k_y=0 meant the wall was at static limit equilibrium.

According to the Fig. 6(b), as the intensity of surcharge is increased, the length of failure wedge in uniform surcharges and limited surcharges becomes greater and smaller, respectively. In fact, as the intensity of surcharge is increased, the tendency to fail from the ends of the width of the surcharge is increased too.

Variations of the yield acceleration coefficient and length of failure wedge against the distance of surcharge from the wall edge are shown in Fig. 7(a) and (b) for different heights. As can be observed, higher walls demonstrated greater yield acceleration in short distances of surcharge from the wall.

Fig. 8(a) shows the variation of internal friction angle of soil versus the yield acceleration coefficient for different distances of surcharge from the wall edge. As can be observed in the

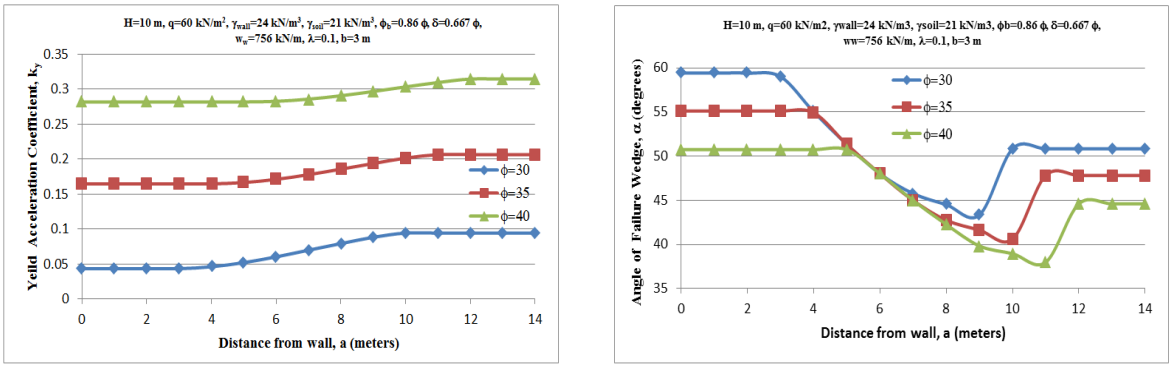

(a) (b)

Fig. 8 (a) Variations of yield acceleration, (b) Variations of angle of failure wedge versus different distances of surcharge from the wall for different internal friction angles of soil

Table 1 Variations of vertical force of earthquake on the yield acceleration for various distances of surcharge from the wall

H=10 m, w_w=756 kN/m, b=3 m, q=60 kN/m^2, ϕ=30, ϕ_b=25.8, δ=20, γ_{wall}=24 60kN/m^3, γ_{soil}=2160kN/m^3			
Yield Acceleration Coefficient, K_y			
Distance from wall, a (meters)	λ=0.1	λ=0	λ=−0.1
0	0.0434	0.0436	0.0438
2	0.0434	0.0436	0.0438
6	0.0602	0.0605	0.0609
8	0.0789	0.0795	0.0801
10	0.0936	0.0945	0.0954
12	0.0936	0.0945	0.0954
14	0.0936	0.0945	0.0954

Table 2 Variations of vertical force of earthquake on the angle of failure wedge for various distances of surcharge from the wall

H=10 m, w_w=756 kN/m, b=3 m, q=60 kN/m^2, ϕ=30, ϕ_b=25.8, δ=20, γ_{wall}=24 60kN/m^3, γ_{soil}=2160kN/m^3			
Angle of Failure Wedge, α (degrees)			
Distance from wall, a (meters)	λ=0.1	λ=0	λ=−0.1
0	59.41	59.41	59.41
2	59.41	59.41	59.41
6	48.01	48.01	48.01
8	44.51	44.51	44.51
10	50.84	50.84	50.84
12	50.84	50.84	50.84
14	50.84	50.84	50.84

figure, an increase in the internal friction angle of the soil caused an increase in the yield acceleration. Also, considering Fig. 8(b), an increase in the internal friction angle of the soil led to an increase in the length of failure wedge.

Considering $\lambda=K_v/K_h$ and trying different values of λ, it can be observed in Tables 1 and 2 that the effect of vertical force of earthquake on the yield acceleration coefficient and angle of failure wedge was very limited and almost negligible.

6. Comparing the results with those reported by other researchers

Among the studies conducted by other researchers, effect of surcharge on the yield acceleration and displacements of the wall has been rarely evaluated. Therefore, in this paper, first, a comparison was made between the results of the proposed method and other works for the condition with surcharge outside the wedge. Indeed, this case behaved like the condition with no surcharge.

Among the analytical techniques, two methods of limit equilibrium and limit analysis were used to obtaine yield acceleration and permanent displacements of retaining walls. Tables 3 and 4 show a comparison between the yield accelerations obtained by limit analysis methods including the studies by Mojallal and Ghanbari (2012), Michalowski (2007), Li *et al*. (2010), the results of which were very satisfactory. Characteristics of Northridge earthquake are given in Fig. 15. Table 5 shows a comparison between the yield accelration obtained by Caltabiano *et al*. (2012) using limit equilibrium theorem. There was a good agreement between the results presented in Table 5.

Table 6 shows a comparison between the angle of failure wedge obtained by Zarrabi-Kashani (1979), Mojallal and Ghanbari (2012), and the proposed method in the current research, representing good consistency between the results. Also, Tables 7 and 8 demonstrate a comparison between the angles of failure obtained by Li *et al*. (2010), Caltabiano *et al*. (2012), and the method proposed in this research.

Table 3 Comparing the k_y obtained by the suggested method and those by Mojallal and Ghanbari (2012), Michalowski (2007)

γ_{wall}=24kN/m^3, γ_s=20kN/m^3, ϕ=30, ϕ_b=30, δ=20, T_w=0.3 m, B_w=0.6H				
k_m Northridge Earthquake[1]	Height of wall H (m)	Yield Acceleration Coefficient, k_y		
		Proposed method	Mojallal and Ghanbari (2012)	Michalowski (2007)
0.344g	3	0.187	0.181	0.180
	5	0.175	0.169	0.169
	7	0.169	0.163	0.163
	10	0.164	0.159	0.159

[1]http://peer.berkeley.edu/smcat/search.html (Fig. 15)

Table 4 Comparing the k_y obtained by the suggested method and that by Li *et al*. (2010)

H=8 m, w_w=556.8kN/m, γ_{wall}=24kN/m^3, γ_s=20kN/m^3, δ=0, λ=0			
ϕ (Degrees)	ϕ_b (Degrees)	Proposed method	Li *et al.* (2010)
25	25	0.0000	0.0000
30	30	0.1119	0.1100
35	35	0.2243	0.2210
40	40	0.3405	0.3400

Table 5 Comparing the k_y obtained by the suggested method with the one by Caltabiano *et al*. (2012)

γ_{wall}=24 kN/m^3, δ=0, λ=0, T_w=0.3 m, B_w=0.6 H					
H (m)	γ_s (kN/m^3)	ϕ (Degrees)	ϕ_b (Degrees)	Yield Acceleration Coefficient, k_y	
				Proposed method	Caltabiano *et al*. (2012)
3	21	30	30	0.0901	0.0910
6	19.5	32	32	0.1351	0.1371
9	19	35	35	0.2030	0.2020

Table 6 Comparing the angle of failure obtained by the suggested method, Mojallal and Ghanbari (2012), Zarrabi-Kashani (1979)

H=10 m, γ_{wall}=24kN/m^3, γ_{soil}=20kN/m^3, β=0, w_w=756 kN/m					
k_h	ϕ (Degrees)	δ (Degrees)	Angle of Failure Wedge, α (degrees)		
			Proposed method	Mojallal and Ghanbari (2012)	Zarrabi-Kashani (1979)
0.2	32	21.33	44.8	46.10	45.80
0.25	34	22.67	43.05	44.78	44.20
0.3	36	24	41.2	43.51	42.60

Table 7 Comparing the angle of failure wedge obtained by the suggested method with the method by Li *et al*. (2010)

H=8 m, w_w=556.8 kN/m, γ_{wall}=24kN/m^3, γ_{soil}=20kN/m^3, δ=0, λ=0			
ϕ (Degrees)	ϕ_b (Degrees)	Angle of Failure Wedge, α (degrees)	
		Proposed method	Li *et al*. (2010)
25	25	57.46	57.90
30	30	56.64	55.20
35	35	52.01	52.02
40	40	49.47	49.50

Table 8 Comparing the angle of failure wedge obtained by the suggested method and that by Caltabiano *et al*. (2012)

γ_{wall}=24kN/m^3, δ=0, λ=0, T_w=0.3 m, B_w=0.6 H					
H (m)	γ_s (kN/m^3)	ϕ (Degrees)	ϕ_b (Degrees)	Angle of Failure Wedge, α (degrees)	
				Proposed method	Caltabiano *et al*. (2012)
3	21	30	30	55.81	55.80
6	19.5	32	32	54.73	54.80
9	19	35	35	53.18	53.21

With regard to the above tables, it can be concluded that the proposed formulation of this research can predict k_y and angle of failure wedge with a satisfactory precision for the condition with no surcharge.

In the studies conducted by previous researchers, effect of surcharge on the yield acceleration and displacements of wall has been rarely investigated. One of these studies was conducted by Caltabiano *et al*. (2012) using the limit equilibrium method.

In order to compare the results of the proposed method with those of Caltabiano *et al*. (2012),

Table 9 Three models used for the purpose of comparison between the suggested method and that by Caltabiano *et al*. (2012)

H=10 m, γ_{wall}=24 kN/m^3, γ_{soil}=18.9 kN/m^3, δ=0, λ=0, w_w=756 kN/m					
model	Type of Surcharge	b (m)	q (kN/m3)	ϕ (Degrees)	ϕ_b (Degrees)
1	Uniform Surcharge	10	20	30	30
2	Uniform Surcharge	6	60	30	30
3	Limited Surcharge	1	189	35	35

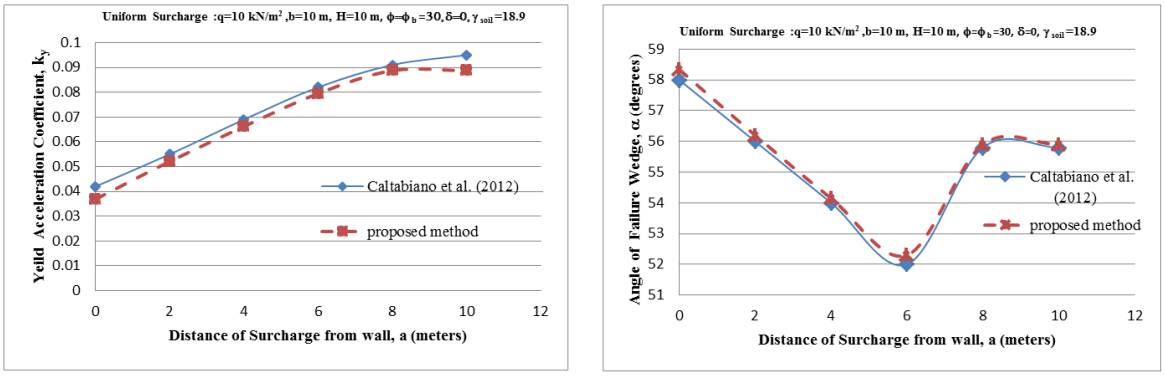

(a) (b)

Fig. 9 Comparison between: (a) Yield acceleration k_v, (b) Angle of failure wedge in the first model between the suggested method and that by Caltabiano *et al*. (2012)

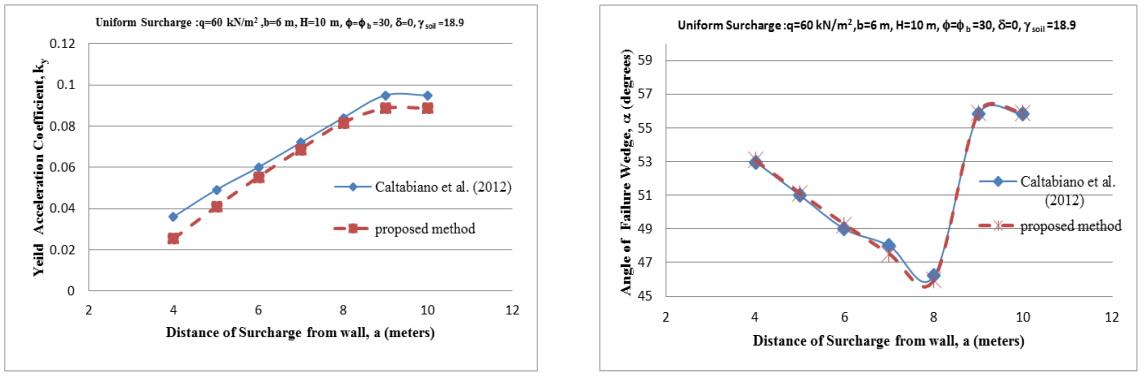

(a) (b)

Fig. 10 Comparison between: (a) Yield acceleration k_v, (b) Angle of failure wedge in the second model between the suggested method and that by Caltabiano *et al*. (2012)

three models with the properties mentioned in Table 9 were considered. Figs. 9 and 10 show the angle of failure wedge and yield acceleration coefficient obtained by the two mentioned methods for the condition with uniform surcharge. Fig. 11 shows a comparison between the results of the suggested method and those reported by Caltabiano *et al*. (2012) for the condition with the surcharge with limited width and limited distance from wall so that the whole surcharge was resting on the plastic wedge of soil. A good agreement can be also observed between the two methods of limit equilibrium and limit analysis.

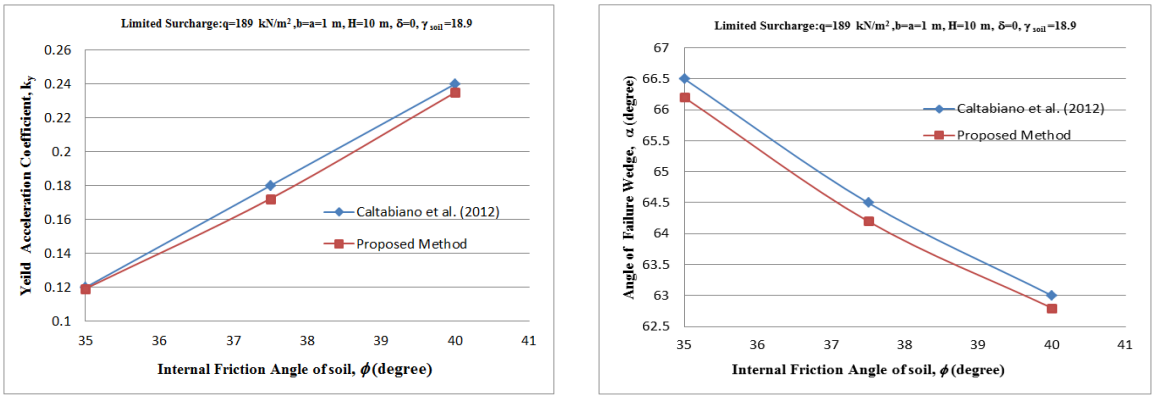

(a) (b)

Fig. 11 Comparison between the proposed method and that by Caltabiano *et al*. (2012) (a) Yield acceleration k_y, (b) Angle of failure wedge in the third model

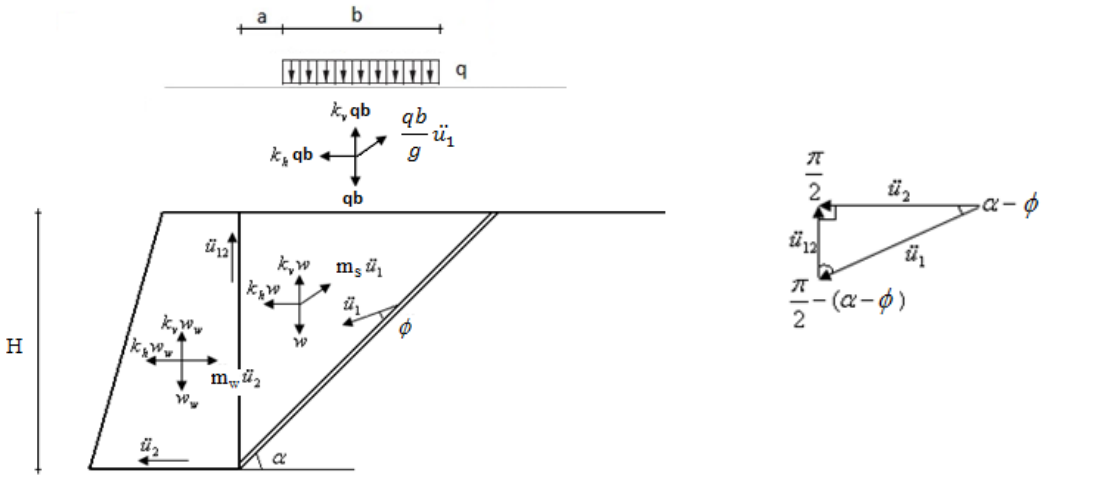

(a) Sliding mechanism (b) Hodograph of the acceleration of sliding mechanism

Fig. 12 Single-block sliding mechanism for surcharge located within the failure wedge

7. Calculations and results of permanent displacement of wall

Once the acceleration of earthquake exceeds the acceleration of structure (k_h>k_y), two mechanisms are likely to occur. In the first mechanism as shown in Fig. 12(a), the wall only experiences sliding failure and moves with $\ddot{u}_2$ acceleration. The block of soil also moves with the acceleration of $\ddot{u}_2$ in this mechanism. In the second mechanism, the wall experiences both sliding and rotational displacements (Fig. 13(a)) and thus the wall and soil block start moving with $\ddot{u}_2$ and $\ddot{u}_1$ accelerations, respectively. It is assumed that the overturning failure is an outward rotation of the wall. . According to the hodographs of Figs. 12 and 13, the kinematic compatibility is satisfied.

In order to calculate the permanent displacement of wall, similar to the calculation of yield acceleration coefficient, three different conditions were considered for the location of surcharge.

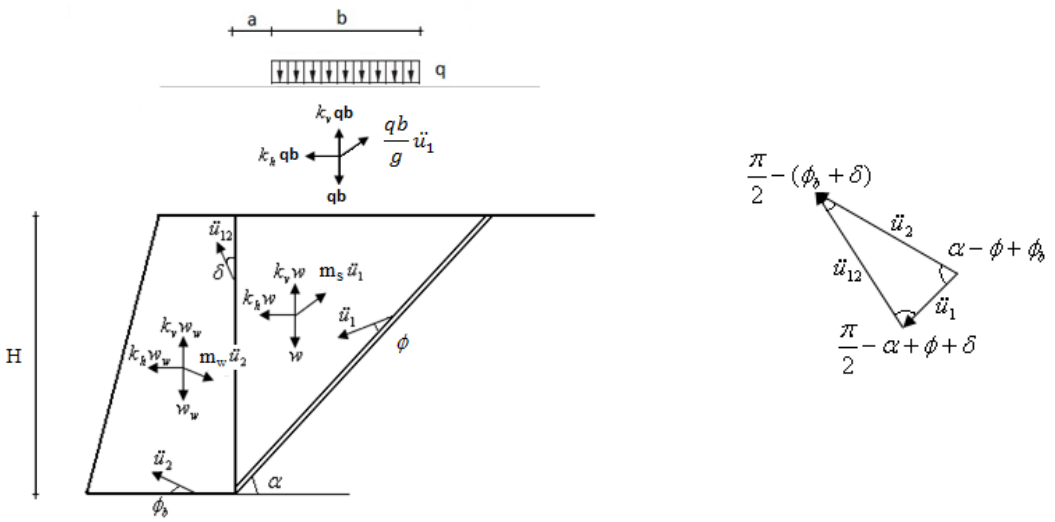

(a) Overturning mechanism

(b) Hodograph of the acceleration of overturning mechanism

Fig. 13 Single-block overturning mechanism for surcharge located within the failure wedge

The used mechanism and forces applied for the condition with surcharge completely inside the failure wedge are shown in Figs. 12 and 13.

In the sliding mechanism, assuming the incompressible wall foundation, the dilatancy angle became zero. This assumption was made because, in granular soils, dilatancy is typically less than that predicted by the associative law (Michalowski 2007). However, in the overturning mechanism, the dilatancy angle became equal to the friction angle.

Rate of the work done by the forces applied to the block interface for the sliding mechanism can be written as

$$\dot{W}_s = K_h W_s V_1 \cos(\alpha-\phi) + (1-K_v)(W_s V_1 \sin(\alpha-\phi)) - m_s \ddot{u}_1 V_1 \tag{21}$$

$$\dot{W}_w = K_h W_w V_2 \cos(\phi_b) - (1-K_v) W_w V_2 \sin(\phi_b) - m_w \ddot{u}_2 V_2 \cos(\phi_b) \tag{22}$$

$$\dot{Q}_1 = K_h qb V_1 \cos(\alpha-\phi) + (1-K_v) qb V_1 \sin(\alpha-\phi) - \frac{qb}{g}\ddot{u}_1 V_1 \tag{23}$$

$$\dot{D} = (\dot{W}_s + \dot{W}_w) + \dot{Q} \tag{24}$$

With regard to Fig. 12(b), the following can be written

$$d' = \frac{\ddot{u}_1}{\ddot{u}_2} = \frac{1}{\cos(\alpha-\phi)} \tag{25}$$

where $\dot{D}$ can be obtained from Eq. (8). By combining Eqs. (21) and (25), the wall acceleration can be obtained from Eq. (26). For simplicity, a part of the equations was denoted by $C_{sliding}$.

$$\ddot{u}_2 = C_{sliding}\left(K_h - K_y\right)$$
$$C_{sliding} = \frac{W_s d\cos(\alpha-\phi) + W_w \cos(\phi_b) + qbd\cos(\alpha-\phi)}{m_w \cos(\phi_b) + m_s dd' + \frac{qb}{g}dd'} \tag{26}$$

In the case of overturning mechanism, forces and the movement direction of soil wedge were similar to the previous case and the difference was in the wall movement and accordingly the direction of the inertial force applied to the wall. Therefore, rate of the work done by the forces applied to the failure wedge and the external force due to the surcharge can be obtained by Eqs. (21) and (23), respectively. Rate of the work done by the forces applied to the wall can be obtained by Eq. (27). Eventually, combining all the equations, acceleration of the wall movement for the overturning mechanism can be written as Eq. (29). For simplicity, a part of the equations was denoted by $C_{overturning}$.

$$\dot{W}_w = K_h W_w V_2 \cos(\phi_b) - (1-K_v) w_w V_2 \sin(\phi_b) - m_w \ddot{u}_2 V_2 \tag{27}$$

$$\frac{\ddot{u}_1}{\ddot{u}_2} = \frac{\cos(\phi_b+\delta)}{\cos(\alpha-\phi-\delta)} \quad \Rightarrow \quad \ddot{u}_1 = d\,\ddot{u}_2 \tag{28}$$

$$\ddot{u}_2 = C_{overturning}\left(K_h - K_y\right)$$
$$C_{overturning} = \frac{W_s d\cos(\alpha-\phi) + W_w \cos(\phi_b) + qbd\cos(\alpha-\phi)}{m_w + m_s d^2 + \frac{qb}{g}d^2} \tag{29}$$

where m_w and m_s are the mass of wall and mass of failure wedge, respectively, $C_{sliding}$ and $C_{overturning}$ are the constants which depend on the wall's geometry, properties of material, and location and intensity of surcharge.

In the condition where only a portion of surcharge was inside the failure wedge, rate of the work done by body forces was similar to the previous case. But, rate of the work due to loading was obtained from Eq. (30). In this case, the wall acceleration can be obtained by Eqs. (31) and (32) for the sliding and overturning mechanisms, respectively.

$$\dot{Q}_2 = (1-K_v)\left[q\left(\frac{H}{\tan(\alpha)} - a\right)V_1 \sin(\alpha-\phi)\right] + K_h q\left(\frac{H}{\tan(\alpha)} - a\right)V_1\cos(\alpha-\phi) - \frac{q}{g}\left(\frac{H}{\tan(\alpha)} - a\right)\ddot{u}_1 V_1 \tag{30}$$

For the sliding mechanisms

$$\ddot{u}_2 = C_{sliding}\left(K_h - K_y\right)$$
$$C_{sliding} = \frac{W_s d\cos(\alpha-\phi) + W_w \cos(\phi_b) + qd\left(\frac{H}{\tan(\alpha)} - a\right)\cos(\alpha-\phi)}{m_w \cos(\phi_b) + m_s dd' + \frac{q}{g}\left(\frac{H}{\tan(\alpha)} - a\right)dd'} \tag{31}$$

For the overturning mechanisms

$$\ddot{u}_2 = C_{overturning}\left(K_h - K_y\right)$$
$$C_{overturning} = \frac{W_s d\cos(\alpha-\phi) + W_w \cos(\phi_b) + qd\left(\frac{H}{\tan(\alpha)} - a\right)\cos(\alpha-\phi)}{m_w + m_s d^2 + \frac{q}{g}\left(\frac{H}{\tan(\alpha)} - a\right)d^2} \tag{32}$$

For the case with surcharge located completely outside the failure wedge, rate of the work done by body forces was similar to first case. Rate of the work done by traction forces due to loading was equal to zero. In this case, the wall acceleration can be obtained by Eqs. (34) and (35) for the sliding and overturning mechanisms, respectively.

$$\dot{Q}_3 = 0 \tag{33}$$

For the sliding mechanisms

$$\ddot{u}_2 = C_{sliding}\left(K_h - K_y\right)$$
$$C_{sliding} = \frac{W_s d\cos(\alpha-\phi) + W_w \cos(\phi_b)}{m_w \cos(\phi_b) + m_s dd'} \tag{34}$$

For the overturning mechanisms

$$\ddot{u}_2 = C_{overturning}\left(K_h - K_y\right)$$
$$C_{overturning} = \frac{W_s d\cos(\alpha-\phi) + W_w \cos(\phi_b)}{m_w + m_s d^2} \tag{35}$$

Eventually, by integrating the wall acceleration twice, the permanent sliding and overturning displacements of wall can be obtained from Eqs. (36) and (37), respectively.

$$u_2 = C_{sliding}\iint\left(K_h - K_y\right)dtdt \qquad V > 0 \quad \text{For sliding mechanism} \tag{36}$$

$$u_2 = C_{overturning}\iint\left(K_h - K_y\right)dtdt \qquad V > 0 \quad \text{For overturning mechanism} \tag{37}$$

In order to calculate the permanent displacement of retating walls, a numerical algorithm (as shown in Fig. 14) can be used. Minimum yield acceleration coefficient and permanent wall displacement for various conditions of surchrage can be calculated by writing a code in a programing language.

Using the proposed formulation, the wall displacement under Northridge-1994 earthquake (Fig. 15) was calculated. The maximum displacement due to two sliding and overturning mechanisms was also considered.

Based on the results illustrated in Fig. 16, the wall displacement for the uniform surcharge and the surcharge with 6 m width were almost equal. Also, in the distances shorter than 4 m from the wall edge, the uniform surcharge and the surcharge with 6 m width underwent large displacements, which led to the wall failure. By making the surcharge distant from the wall edge and exiting the wedge, the displacements became constant.

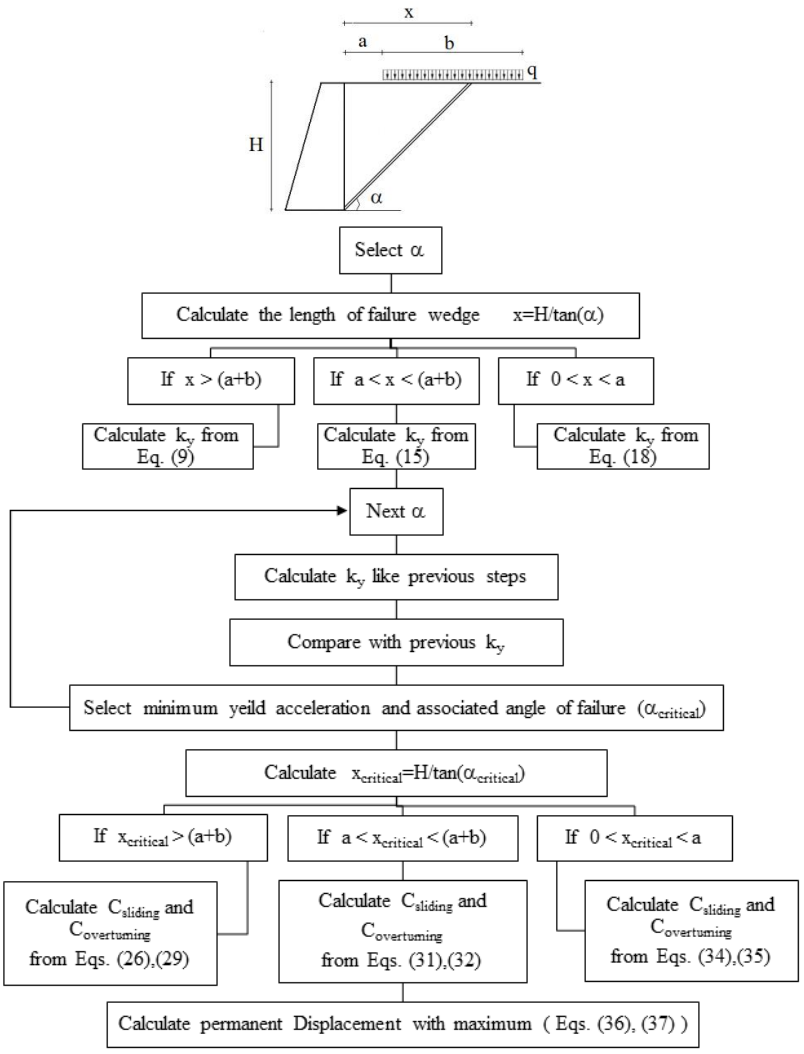

Fig. 14 The algorithm for obtaining permanent displacement of the retaining wall based on the suggested method

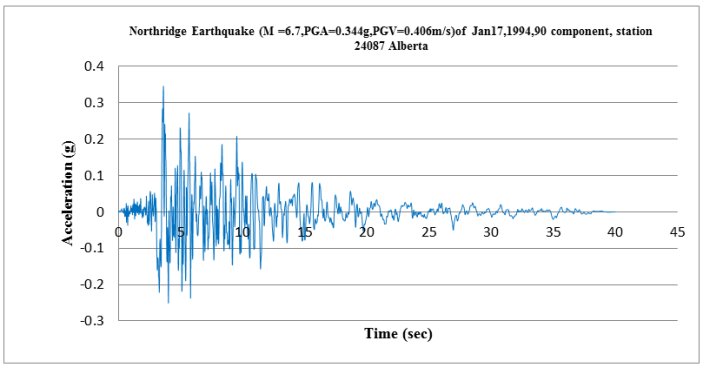

Fig. 15 Northridge earthquake accelerometer (http://peer.berkeley.edu/smcat/search.html)

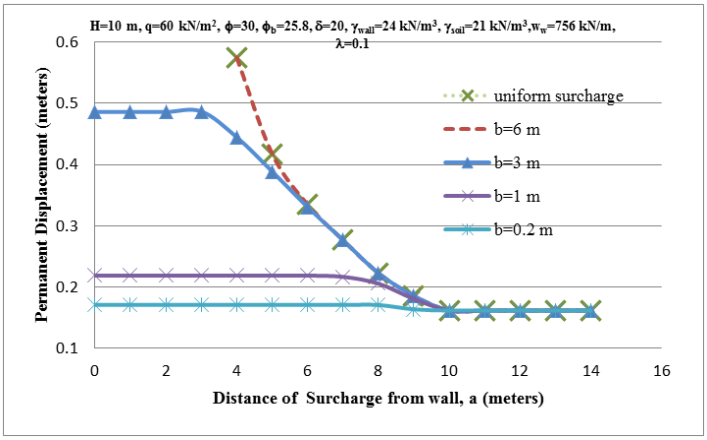

Fig. 16 Variations of permanent displacement of the wall against the distance of surcharge from the end of the wall for different widths of surcharge

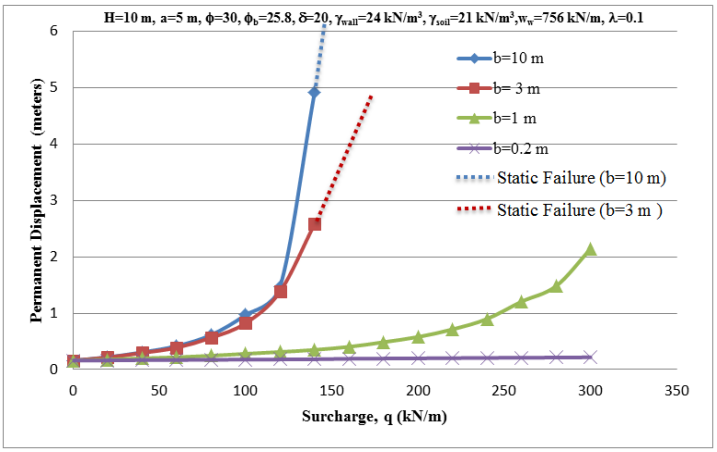

Fig. 17 Variations of permanent displacement against intensity of surcharge for various conditions of surcharge geometry

Fig. 17 shows the trend of increase in the permanent wall displacement against the increase of surcharge. As can be observed, the wall displacement increased by increasing the intensity of surcharge. Also, in the 10 m and 3 m width of the surcharge, with increasing the intensity of surcharge by greater than 150 kN/m^2, the wall underwent static failure and experienced static failure regardless of any earthquakes.

Fig. 18 demonstrates the effect of variations in the height of retaining wall on the permanent displacement of wall for various distances of surcharge from the wall edge. Based on this figure, higher walls showed a greater yield acceleration and smaller displacement for short distances of surcharge from the wall end. In this figure, at the height of 5 m for the surcharges closer than 2.5 m to the wall, the displacements were larger than the allowable values and/or experienced static failure. Therefore, they were plotted as dotted lines. For higher walls, the relative effect of the surcharge (of constant intensity and width) with respect to the wall weight was small; thus, smaller walls for the small values of distance "a" were characterized by smaller k_y (compare with Fig. 7(a))

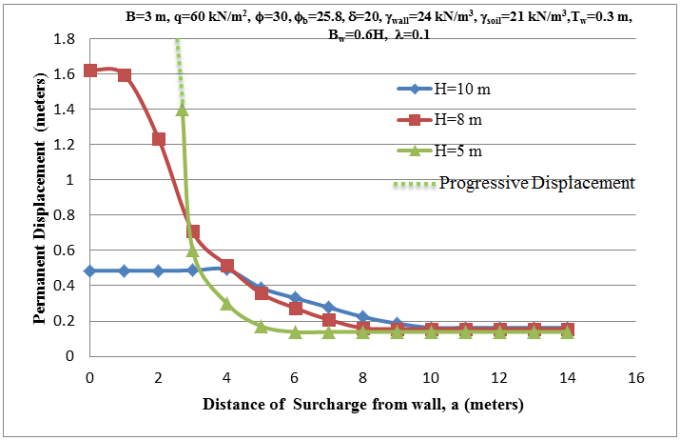

Fig. 18 Variations of permanent displacement of wall against the height of wall for different distances of surcharge from the wall

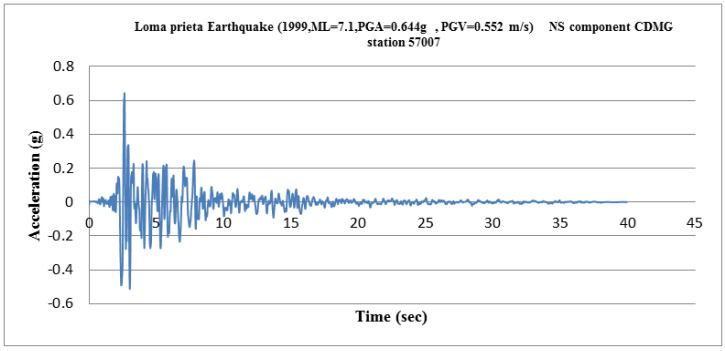

(a)

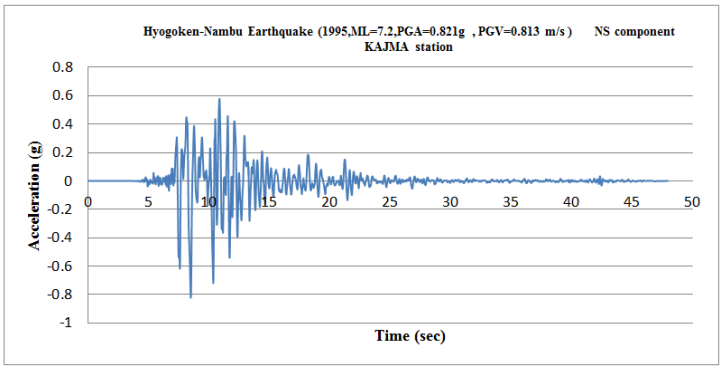

(b)

Fig. 19 (a) Lomaprieta earthquake accelerometer, (b) Hyogoken-Nambu earthquake accelerometer (http://peer.berkeley.edu/smcat/search.html)

and underwent larger displacements than high walls.

Among the studies conducted by other researachers, effect of surcharge on the displacement of retaining walls has been rarely evaluated. Thus, a comparison was made here between the resutls

Table 10 Properties of the two models used for analyses

model	δ (Degrees)	H (m)	β (Degrees)	γ_{wall} (kN/m^3)	ϕ (Degrees)	γ_{soil} (kN/m^3)	w_w (kN/m)	ϕ_b (Degrees)
1	22	4	0	24	33	21.6	130.08	23.3
2	15	8.1	0	24	30	19	669.16	25.8

Table 11 Comparing the obtained permanent displacements with the results of other researchers

	Proposed method	Mojallal and Ghanbari (2012)	Wu (1999)	Proposed method	Mojallal and Ghanbari (2012)	Wu (1999)	Richards and Elms (1979)	Whitman and Liao (1985)
Mechanism	Overturning	Overturning	Sliding and Rocking	Sliding	Sliding	Sliding	_____	_____
k_y	0.098	0.097		0.0978	0.097		0.155	0.1
Displacement	0.153	0.167	0.166	0.1518	0.150	0.062	0.095	0.188

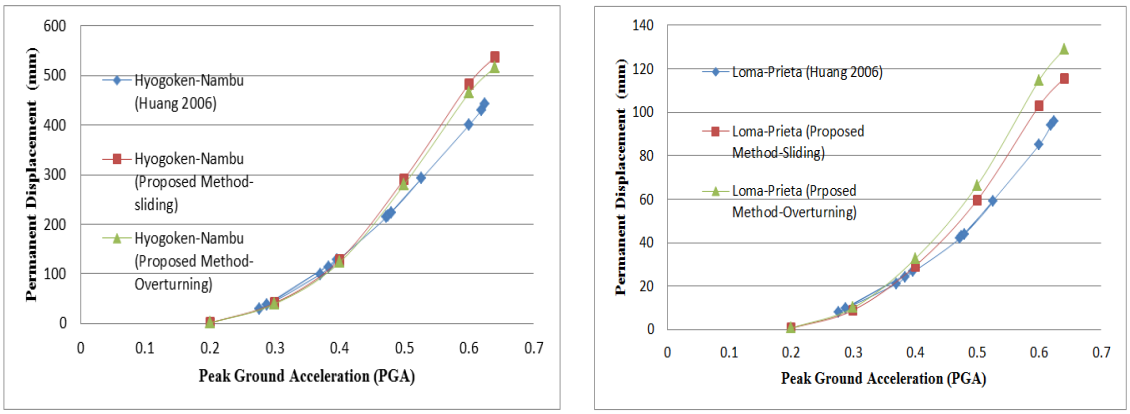

(a) (b)

Fig. 20 Comparing the permanent displacement obtained by the suggested method and the method by Huang (2006) (a) For Hyogoken-nambu earthquake, (b) For Loma prieta earthquake

obtained from the suggested method in this research and those reported by other researachers for the condition with the surcharge located outside the wedge.

In order to compare the displacements obtained from the proposed method with those reported by other researchers, two models were considered. Properties of these models are shown in Table 10. The two models were analyzed and permanent displacement of the retaining wall under different accelerometers (Figs. 19 and 15) was calculated.

Table 11 shows the permanent displacements of the first model obtained by the proposed method and the displacements obtained by Wu (1999), Richards and Elms (1979), Whitman and Liao (1985), and Mojallal and Ghanbari (2012) under the Northridge-1994 earthquake. The displacements obtained by the suggested method and the method by Mojallal and Ghanbari which was based on limit analysis demonstrated a great agreement compared to the results by other techniques which were based on limit equilibrium. The obtained results were an upper bound for the results reported by other researchers.

Fig. 20 shows a comparison between the permanent sliding and overturning displacement of the retaining wall in the second model obtained by the suggested method with the method by Huang (2006). In this case, there was no surcharge on the backfill behind the wall and this model was analyzed under the accelerometers shown in Fig. 19, the acceleration of which was scaled to different values of peak acceleration (e.g., 0.2g, 0.3g, 0.4g, 0.5g, 0.6g, and 0.624g). It can be observed that the results of the proposed technique were somehow greater than those reported by Huang (2006).

Table 12 compares the permanent displacement values obtained by Stamatopoulos *et al*. (2006) and the proposed method. Good agreement was found between the results of the two methods. The displacements of walls were investigated under the parameters of the El-Centro earthquake (1940, ML=6.5, PGA=0.35 g, fundamental period=0.6 s, NS component, http:// www.vibrationdata.com).

Table 12 Comparing the obtained permanent displacements with the results of Stamatopoulos *et al*. (2006)

γ_{soil}=17.7 kN/m^3, δ=3, λ=0, B_w=5 m						
H (m)	W_w (kN/m^3)	ϕ (Degrees)	ϕ_b (Degrees)	permanent displacement		
				Proposed method		Stamatopoulos *et al*. (2006)
				Sliding	overturning	
9	700	26	18	1.7792	1.5159	1.6352
9	700	26	34	0.0084	0.0075	0.0066
9	500	26	46	0.00012	0.00009	0.0001
6	700	26	25	0.0037	0.0035	0.0044
12	700	26	45	0.0058	0.0051	0.0043
9	700	40	27	0.0082	0.0076	0.0067

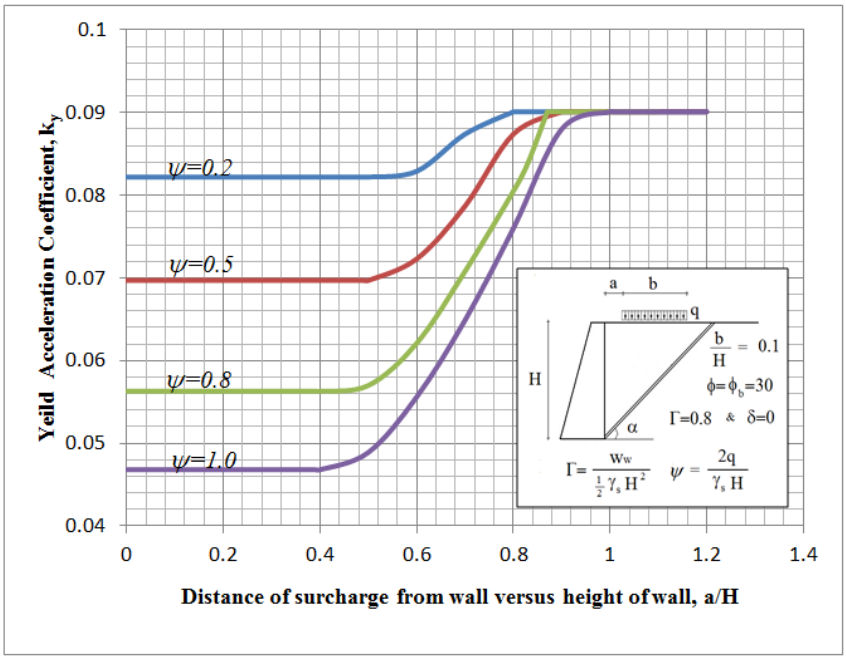

Fig. 21 Design chart of yield acceleration for different distances of surcharge from the wall end with width of surcharge equal to 0.1 H and ϕ=ϕ_b=30

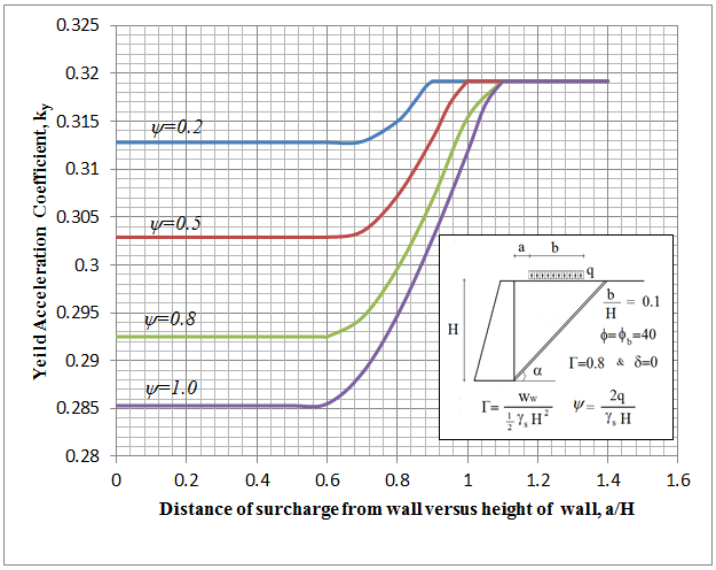

Fig. 22 Design chart of yield acceleration for different distances of surcharge from the wall end with width of surcharge equal to 0.1H and $\phi=\phi_b=40$

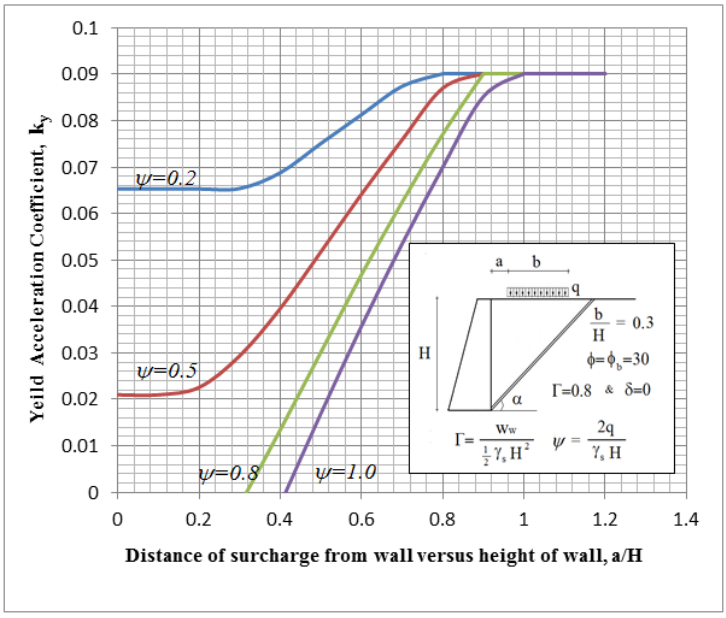

Fig. 23 Design chart of yield acceleration for different distances of surcharge from the wall end with width of surcharge equal to 0.3H and $\phi=\phi_b=30$

8. Design charts based on the proposed method

Design charts with dimensionless parameters are presented in Figs. 21 to 29. The dimensionless parameters were already expressed in Eqs. (38) and (39).

In these equations, Γ is the dimensionless weight of the wall and ψ is dimensionless surcharge factor. Investigating the formulations presented in Section 3, it can be proved that the yield acceleration was a function of dimensionless parameters Γ, ψ, b/H, a/H. By obtaining k_y and α from the following charts, the permanent displacement of wall can be calculated by the maximum values of Eqs. (36) and (37) with considering the special earthquake record.

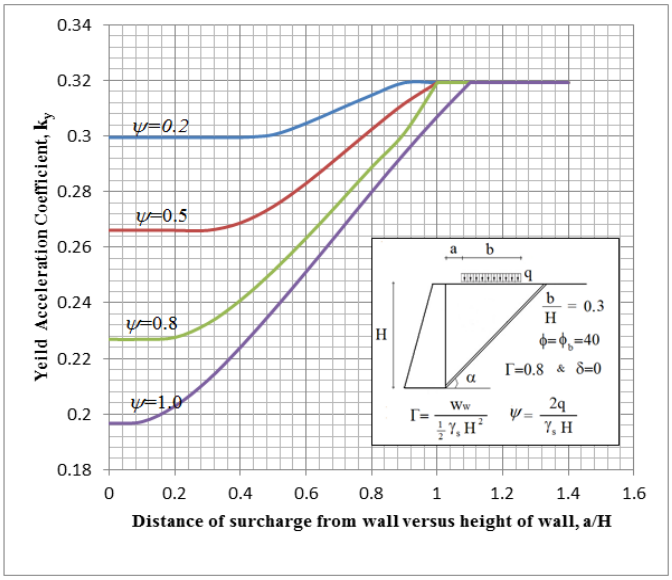

Fig. 24 Design chart of yield acceleration for different distances of surcharge from the wall end with width of surcharge equal to 0.3H and $\phi=\phi_b=40$

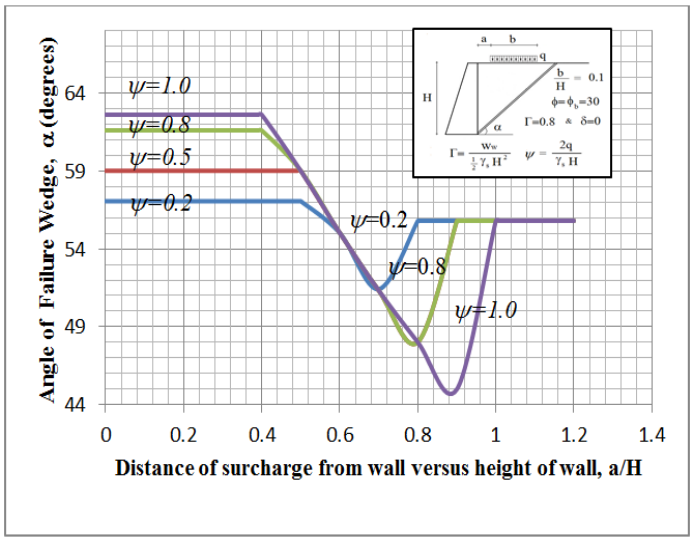

(a) $\phi=\phi_b=30$

Fig. 25 Design chart of angle of failure wedge for different distances of surcharge from the wall end with width of surcharge equal to 0.1H and (a) $\phi=\phi_b=30$, (b) $\phi=\phi_b=40$

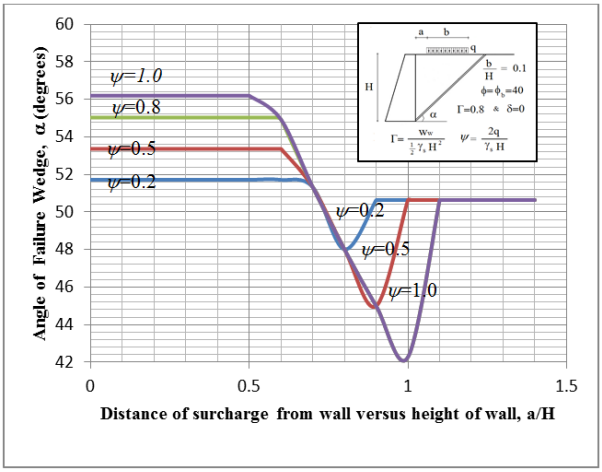

(b) $\phi=\phi_b=40$

Fig. 25 Continued

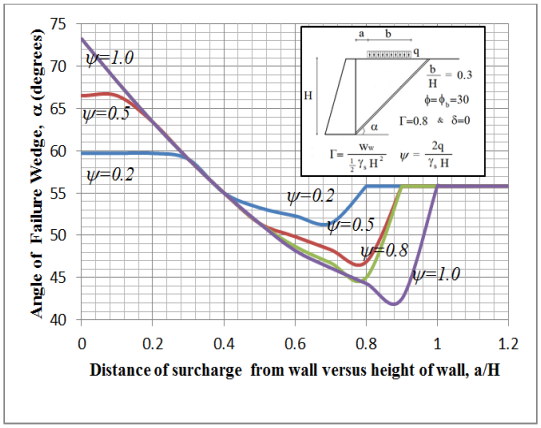

(a) $\phi=\phi_b=30$

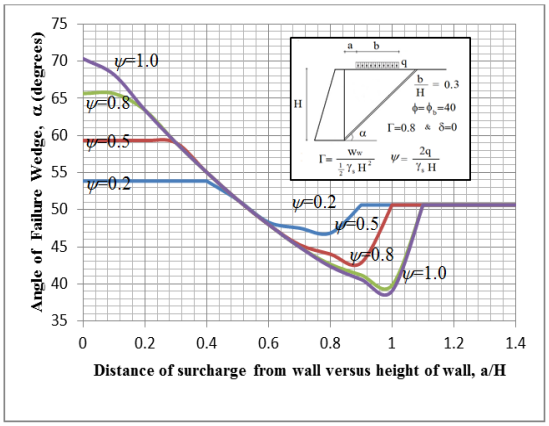

(b) $\phi=\phi_b=40$

Fig. 26 Design chart of angle of failure wedge for different distances of surcharge from the wall end with width of surcharge equal to 0.3H and: (a) $\phi=\phi_b=30$, (b) $\phi=\phi_b=40$

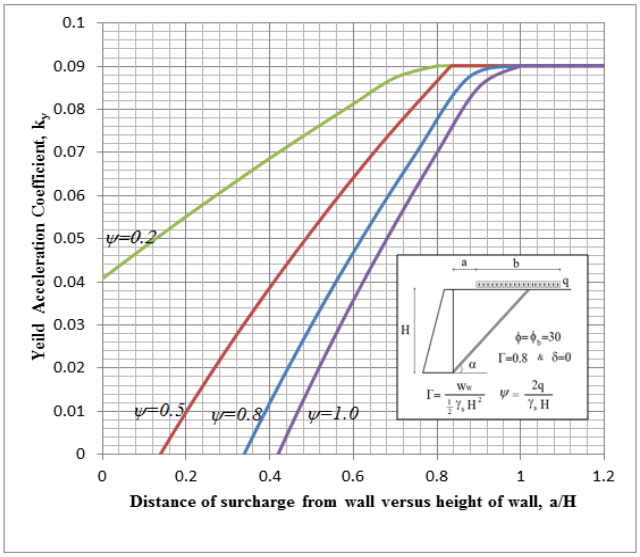

Fig. 27 Design chart of yield acceleration for different distances of uniform surcharge from the wall end, $\phi=\phi_b=30$

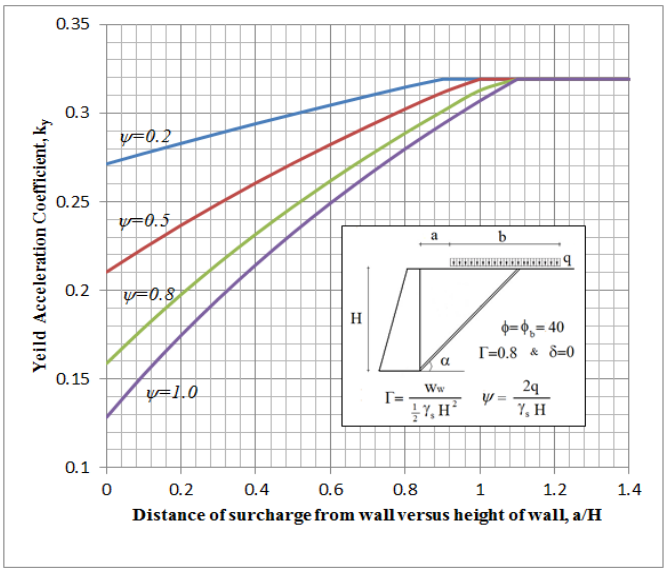

Fig. 28 Design chart of yield acceleration for different distances of uniform surcharge from the wall end, $\phi=\phi_b=40$

If the mentioned ratios were equal for two arbitrary walls, those walls would have equal yield accelerations. If a part of the surcharge was outside the failure wedge, then that surcharge would act like a uniform surcharge. In other words, the width of surcharge had no effects on the solution. Therefore, the b/H ratio was not effective for uniform surcharges. In plotting the design charts, first, a limited surcharge was studied and then the charts for uniform surcharge were presented. For the condition with limited surcharge inside the failure wedge, two widths of 0.1H and 0.3H were

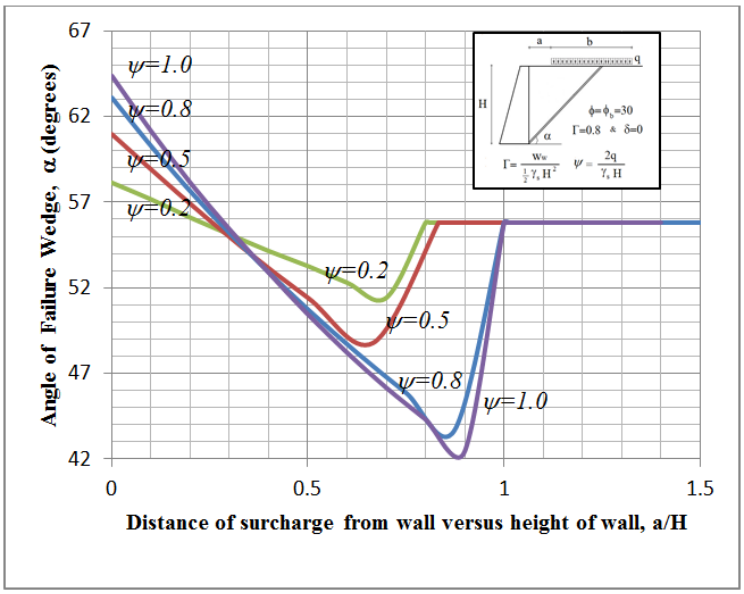

(a) $\phi=\phi_b=30$

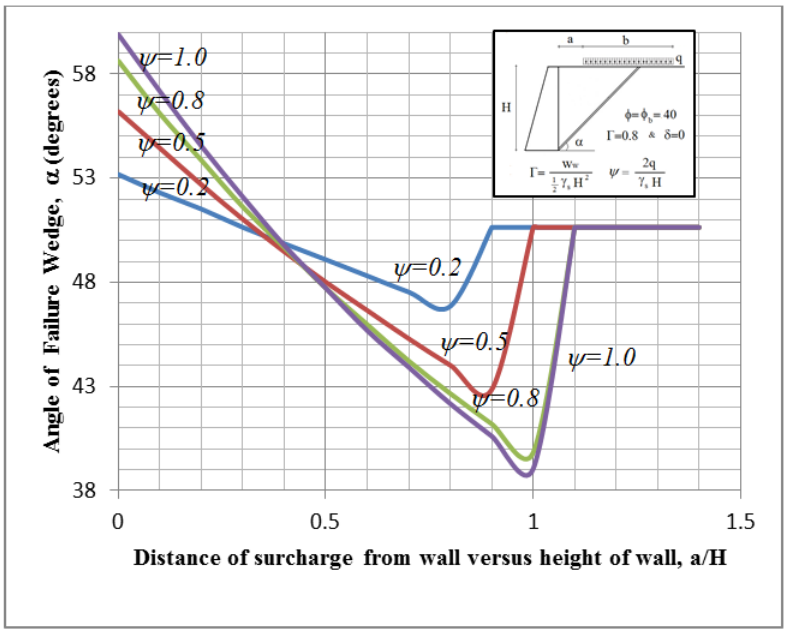

(b) $\phi=\phi_b=40$

Fig. 29 Design chart of angle of failure wedge for different distances of uniform surcharge from the wall end: (a) $\phi=\phi_b=30$, (b) $\phi=\phi_b=40$

presented. For the surcharges with the widths greater than the mentioned values, the wall behavior was similar to the condition with uniform surcharge and thus the design charts for uniform surcharge can be used. For the case not reproduced in the design charts, the proposed algorithms or the closed-form solutions presented by Caltabiano *et al*. (2000, 2012) can be applied.

9. Conclusions

In this paper, using the upper bound theorem of limit analysis and presenting a new formulation, permanent displacement, critical angle of failure, and yield acceleration were obtained for the cantilever and gravitational retaining walls in the vicinity of a surcharge. In this method, soil properties such as dilation angle, associated flow rule, geometry of the model as well as intensity and location of surcharge with regard to the wall were considered in calculating displacements. In calculating the permanent displacement of retaining wall, two sliding and overturning mechanisms were considered.

The results obtained from the proposed method showed that, if the surcharge was close to the wall edge, higher walls showed greater yield accelerations and smaller displacements. Also, an increase in the intensity of surcharge caused a decrease in yield acceleration and increase in the wall displacements. However, by increasing the intensity of surcharge, the angle of failure wedge can both increase or decrease, depending on the width of surcharge and surcharge location. This research showed that, by making the surcharge away from the wall edge, the yield acceleration increased and angle of failure wedge and permanent displacements decreased. With increasing the distance of the surcharge from the wall, the surcharge effect finally disappeared and the wall performed as the case without the surcharge.

The results obtained from the proposed method represented that, by increasing the internal friction angle of soil, the yield acceleration increased and the permanent displacements of the retaining wall decreased. Variations in the vertical force of earthquake did not have a significant effect on the wall displacements. Finally, design charts were presented for the quick estimation of yield acceleration and angle of failure wedge.

References

Anastasopoulos, I., Georgarakos, T., Georgiannou, V., Drosos, V. and Kourkoulis, R. (2010), "Seismic performance of bar-mat reinforced-soil retaining wall: shaking table testing versus numerical analysis with modified kinematic hardening constitutive model", *Soil Dyn. Earthq. Eng*., **30**(10), 1089-1105.

Biondi, G., Maugeri, M. and Cascone, E. (2009), "Performance-based pseudo-static analysis of gravity retaining walls", *Proceedings of the International Conference on Performance-based design in Earthquake Geotechnical Engineering*, Tokyo, Japan.

Biondi, G., Cascone, E. and Maugeri, M. (2014), "Displacement versus pseudo-static evaluation of the seismic performance of sliding retaining walls", *Bull. Earthq. Eng.*, **12**(3), 1239-1267.

Caltabiano, S., Cascone, E. and Maugeri, M. (1999), "Sliding response of gravity retaining walls", *Proceedings of the2nd International Conference on Earthquake Geotechnical Engineering*, Lisbon, Portugal.

Caltabiano, S., Cascone, E. and Maugeri, M. (2000), "Seismic stability of retaining walls with surcharge", *Soil Dyn. Earthq. Eng*., **20**(5-8), 469-76.

Caltabiano, S., Cascone, E. and Maugeri, M. (2005), "A procedure for seismic design of retaining walls", *Seismic Prevention of Damage: A Case Study in a Mediterranean City*, Ed. Maugeri, M., WIT Press.

Caltabiano, S., Cascone, E. and Maugeri, M. (2012), "Static and seismic limit equilibrium analysis of sliding retaining walls under different surcharge conditions", *Soil Dyn. Earthq. Eng*., **37**, 38-55.

Chen, W.F. (1975), *Limit Analysis and Soil Plasticity*, Elsevier, Amsterdam.

Chen, W.F. and Liu, X.L. (1990), *Limit Analysis in Soil Mechanics*, Elsevier, Amsterdam.

Cocco, L., Suarez, L.E. and Matheu, E.E. (2010), "Development of a nonlinear seismic response capacity spectrum method for intake towers of dams", *Struct. Eng. Mech.*, **36**(3), 321-341.

Drucker, D.C., Prager, W. and Greenmberg, H.G. (1952), "Etended limit design theorems for continuous media", *Quart. J. Mech. Appl*. Math., **9**, 381-389.
Durand, A.F., Vargas, Jr E.A. and Vaz, L.E. (2006), "Applications of numerical limit analysis (NLA) to stability problems of rock and soil masses", *Int. J. Rock Mech. Min. Sci*., **43**, 408-425.
Evangelista, A., Scotto di Santolo, A. and Simonelli, A.L. (2010), "Evaluation of pseudo static active earth pressare coefficient of cantilever retaining walls", *Soil Dyn. Earthq. Eng*., **30**, 1119-28.
Fang, Y.S., Yang, Y.C. and Chen, T.J. (2003), "Retaining wall damaged in the Chi–Chi earth- quake", *Can. Geotech. J.*, **40**, 1142-1153.
Feinberg, S.M. (1948), *The Principle of Limiting Stresses*, Prnkl Mat Mech. (in Russian)
Finn, W.D.L. (1967), "Application of limit plasticity in soil mechanics", *J. Soil Mech. Found. Div.*,ASCE, **93**(5), 101-120.
Ghanbari, A. and Taheri, M. (2012), "An analytical method for calculating active earth pressure in reinforced retaining walls subject to a line surcharge", *Geotext. Geomembrain*., **34**,1-10.
Greco, VR. (2006), "Active thrust due to backfill subject to lines of surcharge", *J. Geotech. Geoenvir. Eng*., ASCE, **132**, 269-271.
Gursoy, S. and Durmus, A. (2009), "Investigation of linear and nonlinear of behaviours of reinforced concrete cantilever retaining walls according to the earthquake loads considering", *Struct. Eng. Mech*., **31**(1), 75-91.
Haciefendioglu, K., Bayraktar, A. and Turker, T. (2010), "Seismic response of concrete gravity dam-ice covered reservoir-foundation interaction systems", *Struct. Eng. Mech*., **36**(4), 499-511.
Hill, R. (1948), "A variational principle of maximum plastic work in classical plasticity", *Quart. J. Mech. Appl. Math*., **1**, 18-28.
Hill, R. (1951), "On the state of stress in a plastic-rigid body at the yield point", *Philos. Mag*., **42**, 868-875.
Huang, C.C. and Chen, Y.H. (2004), "Seismic stability of soil retaining walls situated on slope", *J. Geotech. Geoenvir. Eng.*, ASCE, **130**(1), 45-57.
Huang, C.C. (2006), "Seismic displacement analysis of free-standing highway bridge abutment", *J. GeoEng*., **1**(1), 29-39.
Huang, C.C., Wu, S.H. and Wu, H.J. (2009), "Seismic displacement criterion for soil retaining walls based on soil strength mobilization", *J. Geotech. Geoenvir. Eng.*, ASCE, **135**(1), 76-82.
Kim, T.H., Kim, Y.J. and Shin, H.M. (2008), "Seismic performance assessment of reinforced concrete bridge piers supported by laminated rubber bearings", *Struct. Eng. Mech*., **29**(3), 259-278.
Kloukinas, P. and Mylonakis, G. (2011), "Rankine solution for seismic earth pressures on L-shaped retaining walls", *Proceedings of the 5th International Conference on Earthquake Geotech- nical Engineering*, Santiago, Chile, paper No. RSSKL.
Li, X., Wu, Y. and He, S. (2010), "Seismic stability analysis of gravity retaining walls", *Soil Dyn. Earthq. Eng.*, **30**, 875-878.
Michalowski, R.L. (1998a), "Limit analysis in stability calculations of reinforced soil structures", *Geotext. Geomembrain*., **16**, 311-31.
Michalowski, R.L. (1998b), "Soil reinforcement for seismic design of geotechnical structures", *Comput. Geotech*., **23**(1-2), 1-17.
Michalowski, R.L. and You, L. (2000), "Displacements of reinforced slopes subjected to seismic loads", *J. Geotech. Geoenvir. Eng*., ASCE, **126**(8), 685-94.
Michalowski, R.L. (2007), "Displacement of multiblock geotechnical structures subjected to seismic excitation", *J. Geotech. Geoenvir. Eng.*, ASCE, **133**(11), 1432-1439.
Michalowski, R.L. (2010), "Limit analysis and stability charts for 3D slope failures", *J. Geotech. Geoenvir. Eng.*, ASCE, **136**(4), 583-93.
Mojallal, M. and Ghanbari, A. (2012), "Prediction of seismic displacements in gravity retaining walls based on limit analysis approach", *Struct. Eng. Mech*., **42**(2), 247-267.
Mononobe, N. and Matsuo, H. (1929), "On the determination of earth pressures during earthquakes", *Proceedings of the World Engineering Congress*, Tokyo, Japan.
Motta, E. (1994), "Generalized Coulomb active-earth pressure for distanced surcharge", *J. Geotech Eng.*,

ASCE, **120**(6), 1072-9.
Mylonakis, G., Kloukinas, P. and Papantonopoulos, C. (2007), "An alternative to the Mononobe–Okabe equations for seismic earth pressures", *Soil Dyn. Earthq. Eng*., **27**, 957-69.
Nadim, F. (1982), "A numerical model for evaluation of seismic behavior of gravity retaining walls", ScD Thesis, Research report R82-33, Department of Civil Engineering, Massachusetts Institute of Technology.
Nadim, F. and Whitman, R.V. (1983), "Seismically induced movement of retaining walls", *J. Geotech. Eng.*, ASCE, **109**(7), 915-931.
Newmark, N.M. (1965), "Effects of earthquakes on dams and embankments", *Geotechnique*, **15**(2), 139-159.
Okabe, S. (1924), "General theory on earth pressure and seismic stability of retaining wall and dam", *J. Japan Soc. Civil Eng*., **10**(6), 1277-1323.
Pitilakis, K. and Moutsakis, A. (1989), "Seismic analysis and behaviour of gravity retaining walls - the case of Kalamata harbour quaywall", *Soil. Found.*, **29**(1), 1-17.
Richards, R. and Elms, D.G. (1979), "Seismic behavior of gravity retaining walls", *J. Geotech. Eng. Div*., **105**(4), 449-464.
Tateyama, M., Tatsuoka, F., Koseki, J. and Horii, K. (1995), "Damage to soil retaining walls for railway embankments during the Great Hanshin-Awaji Earthquake", *Proceedings of the 1st International Conference on Earthquake Geotechnical Engineering*, Tokyo.
Sadrekarimi, A., Ghalandarzadeh, A. and Sadrekarimi, J. (2008), "Static and dynamic behavior of hunchbacked gravity quay walls", *Soil Dyn. Earthq. Eng*., **28**(2), 99-117.
Stamatopoulos, CA., Velgaki, E.G., Modaressi, A. and Lopez-Caballero, F. (2006), "Seismic displacements of gravity walls by a two-body model", *Bull. Earthq. Eng.*, **4**, 295-318.
Trandafir, A.C., Kamai, T. and Sidle, R.C. (2009), "Earthquake induced displacements of gravity walls and anchor-reinforced walls", *Soil Dyn. Earthq. Eng*., **29**, 428-437.
Varzaghani, M.I. and Ghanbari, A. (2014), "A new analytical model to determine dynamic displacement of foundations adjacent to slope", *Geomech. Eng.*, **6**(6), 561-575.
Whitman, R.V. and Liao, S. (1985), "Seismic design of retaining walls", Miscellaneous paper GL-85-1, Department of the Army, US Army Corps Engineers, Washington, DC.
Wu, Y. (1999), "Displacement-based analysis and design of rigid retaining walls during earthquake", PhD Dissertation, Univ. of Missouri-Rolla.
Wu, Y. and Prakash, S. (2001), "Seismic displacement of rigid retaining walls - state of the art", *Proceedings of the Fourth International Conference on Recent Advances in Geotechnical Earthquake Engineering and Soil Dynamics*, San Diego, California, March.
You, L. and Michalowski, R.L. (1999), "Displacement charts for slopes subjected to seismic loads", *Comput. Geotech*., **25**(1), 45-55.
Yu, H.S. (2006), *Plasticity and Geotechnics*, Springer Science + Business Media LLC.
Yang, X.L. (2007), "Upper bound limits analysis of active earth pressure with different fracture surface and nonlinear yield criterion", *Theo. Appl. Frac. Mech*., **47**(1), 46-56.
Zarrabi-Kashani, K. (1979), "Sliding of gravity retaining wall during earthquakes considering vertical accelerations and changing inclination of failure surface", M.S. Thesis, Department of Civil Engineering, Massachusetts Institute of Technology.

CC

Nomenclature

α	angle of the slip plane to the horizontal	H	height of the retaining wall
β	slope angle of the retained soil	A	Distance of Surcharge from wall

$\gamma_s=\gamma_{soil}$	soil unit weight	B	Width of Surcharge
γ_{wall}	wall unit weight	X	Length of Failure Wedge
δ	friction angle between soil and wall	W_s	weight of the soil plastic wedge
ϕ	Internal friction angle	W_w	weight of the wall
ϕ_b	friction angle between the foundation soil and the wall base	m_s	Mass of the soil plastic wedge
c	cohesion of the soil	M_w	Mass of the wall
k_h	horizontal seismic coefficient	Q	Surcharge
K_v	vertical seismic coefficient	$\dot{D}$	The rate of internal work
K_y	Yield Acceleration Coefficient	$\dot{W}_s$	the rate of external work for weight of the soil
λ	The ratio of vertical to horizontal seismic coefficient	$\dot{W}_w$	the rate of external work for weight of the wall
V_1	velocity vector of the failure wedge	$\dot{Q}_1$	the rate of external work for the Surcharge in one status
V_2	velocity vector of the retaining wall	$\dot{Q}_2$	the rate of external work for the Surcharge in two status
V_{12}	relative velocity between the wall and failure wedge	K_{y1}	Yield Acceleration Coefficient in one status
$\ddot{u}_1$	acceleration vector of the failure wedge	K_{y2}	Yield Acceleration Coefficient in two status
$\ddot{u}_2$	acceleration vector of the retaining wall	K_{y3}	Yield Acceleration Coefficient in three status
$\ddot{u}_{12}$	relative acceleration between the wall and failure wedge	$C_{sliding}$	Sliding Constant coefficient
T_w	Top wide of the wall	$C_{overturning}$	Overturning Constant coefficient
B_w	Bottom wide of the wall	Γ	dimensionless weight of the wall
		ψ	dimensionless surcharge factor